THE JOURNAL OF PHYSICAL CHEMISTRY B

ARTICLE

pubs.acs.org/JPCB

Forced Unbinding of Individual Urea−Aminotriazine Supramolecular Polymers by Atomic Force Microscopy: A Closer Look at the Potential Energy Landscape and Binding Lengths at Fixed Loading Rates

Anika Embrechts,[†] Holger Schönherr,*[,‡] and G. Julius Vancso*

Department of Materials Science and Technology of Polymers and MESA[+] Institute for Nanotechnology, University of Twente, Post Office Box 217, 7500 AE Enschede, The Netherlands

ABSTRACT: Atomic force microscopy-based single-molecule force spectroscopy (AFM-SMFS) was used to study the forced unbinding of quadruple self-complementary hydrogen-bonded urea−aminotriazine (UAT) complexes in hexadecane (HD). To elucidate the bond strength of individual linkages the unbinding forces of UAT supramolecular polymers were investigated for the first time. The bond rupture was probed at three different, fixed piezo retraction rates in far from equilibrium conditions. The number of supramolecular bonds (N) between AFM tip and the surface was determined by independent knowledge of the linker length. The observed rupture force of urea−aminotriazine (UAT)-based supramolecular polymer chains was found to decrease with increasing rupture length. The dependence of the most probable rupture force on N was in quantitative agreement with the theory of uncooperative bond rupture for supramolecular linkages switched in series. Experiments with three different, fixed loading rates provided identical values (within the experimental error) for the characteristic bond length x_β and the off-rate constant in the absence of force $k_{off}(f = 0)$. The value of x_β was found to agree with literature data on the hydrogen-bond distance obtained via crystallographic data of the hydrogen-bonded dimer. This work broadens the scope of our previous report showing that relevant parameters of the bond energy landscape can be derived from a single data set of rupture events at a fixed loading rate for supramolecular linkages switched in series.

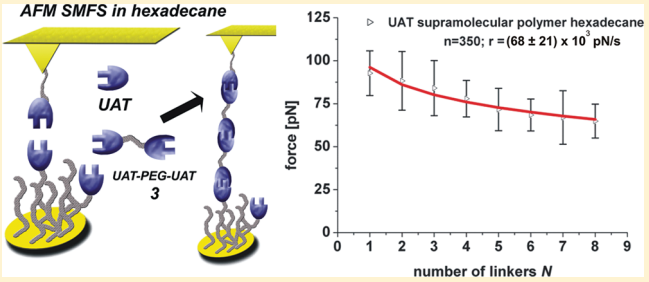

INTRODUCTION

Self-assembly of supramolecular structures into higher-order hierarchical assemblies, for instance, mediated by hydrogen bonding, has received tremendous attention in nanotechnology, sensing, biochemistry, and biophysics. Hydrogen-bonded polymers, which are abundant in nature, are also key to the development of synthetic self-healing materials.[1] Such materials, which are based on the directional recognition of designed hydrogen-bonded moieties, may provide an avenue toward long-lasting self-repairing materials.

In the last two decades, advanced nanoscale characterization tools have emerged that enable one to study the underlying spontaneous self-assembly processes on the molecular level.[2] These techniques comprise, among others, optical[3]/magnetic tweezers,[4] the biomembrane force probe[5] and atomic force microscopy-based single-molecule force spectroscopy (AFM-SMFS).[2,6,7] The corresponding studies provided astonishing new insights into the structure and function of many proteins, as well as their folding mechanisms, as was recently demonstrated by the groups of Gaub[7] and Samori.[8]

To obtain a more thorough insight into the function and strength of hydrogen-bonded systems on a molecular level, we synthesized supramolecular model compounds and studied their bond strength by AFM-SMFS. In particular, we investigated the bond strength of 2-ureido-4[1H]-pyrimidinone (UPy)[9] dimers as well as a urea−aminotriazine (UAT)-based complementary quadruple hydrogen-bonded motif in hexadecane (HD) on a molecular level,[10] using the loading rate dependence of rupture forces described by the Kramers−Bell−Evans model.[11]

In general, the Kramers−Bell−Evans approach (eq 1) is applied to study the potential energy landscape via the loading rate dependence of the most probable rupture force f^* of ligand−receptor interactions:

$$f^* = f_\beta \ln\left(\frac{r_f}{r_f^0}\right) \quad (1)$$

From the thermal scale force f_β, the loading rate r_f, and the loading rate at zero force r_f^0, the bond lifetime $t_{off}(0)$ [or the off-rate $k_{off}(0) = 1/t_{off}(0)$] can be determined:

$$t_{off}(0) = \frac{f_\beta}{r_f^0} \quad (2)$$

More recently we reported on a new approach, which directly yields all parameters of the potential energy landscape on the basis of only one single data set acquired at one *fixed* loading rate.[12]

Received: September 16, 2011
Revised: November 13, 2011
Published: November 16, 2011

Scheme 1. Synthesis of Bis(UAT)PEG Donor−Acceptor−Donor−Acceptor Linker for Formation of Supramolecular Hydrogen-Bonded Polymers Based on Urea−Aminotriazine Units

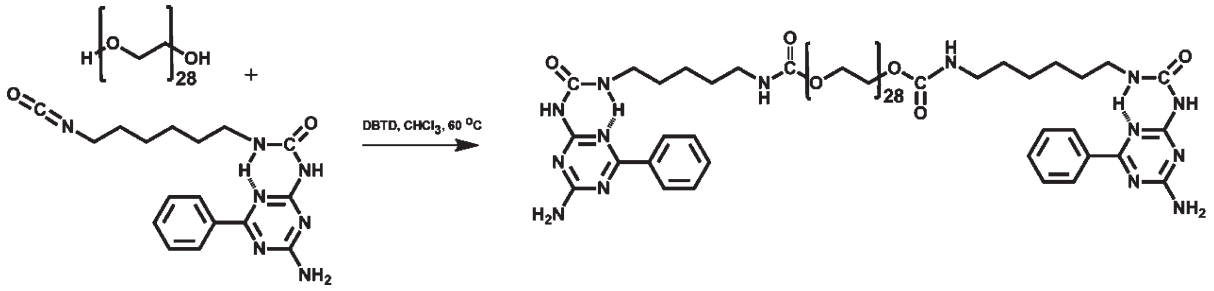

This approach, which was applied to supramolecular polymers of UPy in HD,[9] relies on the extended Evans model for ligand−receptor interactions switched in series.[13] Williams and Evans[13] predicted the decrease of f^* as a function of the numbers of linkers N switched in series for uncooperative bond rupture:

$$f^* = f_\beta(\ln r_f - \ln N] = f^*_{\text{single}} - f_\beta \ln N \qquad (3)$$

Using computer simulations, Fugman and Sokolov[14] also reported the nonmonotonic dependence of polymer rupture force for small N.

Here we report on the validation of this approach and the determination of the characteristic bond length in UAT complexes based on an extensive study of the unbinding forces of UAT-based self-complementary supramolecular hydrogen-bonding polymers in HD. In addition to probing UAT supramolecular polymers, the independence of the estimated parameters that characterize the corresponding energy landscape from the choice of the (fixed) loading rate is shown.

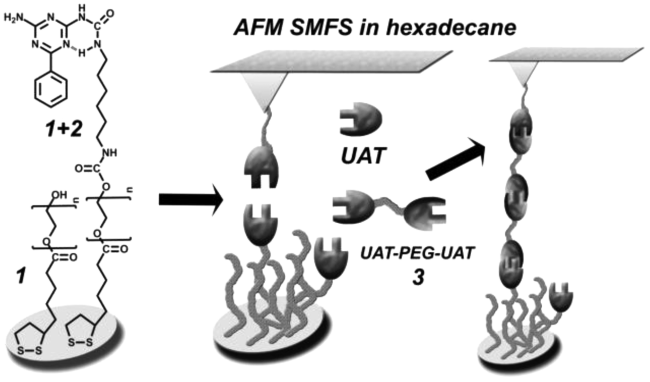

Figure 1. Schematic of AFM-SMFS of supramolecular UAT polymers in hexadecane. A gold-coated surface and a gold-coated AFM probe are functionalized with PEG **1** and PEG−UAT **1** + **2** moieties. The bifunctional UAT−PEG linker **3** is added to the solution to form supramolecular polymers.

MATERIALS AND METHODS

Materials. Anhydrous hexadecane (purity ≥99%, water <0.005%) and dibutyltin dilaurate were purchased from Sigma−Aldrich (Steinheim, Germany) and used as received. Chloroform (stabilized with amylene) and dichloromethane were purchased from Biosolve (Valkenswaard, The Netherlands). 1,2-Dithiolane-3-pentyl-derivatized poly(ethylene glycol) (PEG) **1**, 1-(4-amino-6-phenyl-1,3,5-triazin-2-yl)-3-(6-isocyanatohexyl)urea (UAT) **2**, and PEG-linked bis(urea-aminotriazine) **3** were synthesized according to published procedures.[9,15] PEG-linked bis(urea−aminotriazine) was synthesized by use of 1.0525 g of PEG_{28} (Polypure 95% pure PEG_{28}, M_w = 1251.5 g/mol; 0.8 mmol), which was previously dried three times by azeotropic distillation over anhydrous toluene. Excess 1-(4-amino-6-phenyl-1,3,5-triazin-2-yl)-3-(6-isocyanatohexyl)urea **2** (1.2330 g, 3.5 mmol), 2 drops of the catalyst dibutyltin dilaurate, and 40 mL of dry chloroform were added under nitrogen environment. The clear solvent mixture was heated to 60 °C and the reaction was left stirring overnight under argon atmosphere. After 20 h of reaction time, 2.5 g of silica (Kieselgel 60) and 2 drops of catalyst were added to remove unreacted isocyanate end-functionalized urea−aminotriazine. The reaction was continued for 6 h, after which no residual isocyanate peak could be detected via Fourier transform infrared spectroscopy (FT-IR). After cooling down, the silica-bound material was removed by washing the reaction mixture with chloroform over a glass filter. Chloroform was removed by rotation evaporation and the residue was further dried under vacuum for several hours and stored under argon atmosphere. Isolated yield: 66.4% (1.40 g). ^{1}H NMR (300 MHz, $CDCl_3$): δ 10.29 (s, 2H, NH/N H-bond), 9.90 (s, 2H, NH/N intra H-bond), 9.33 [s, 2H, NH (from NH_2)/N H-bond], 8.20 (d, 4H, ortho), 7.60−7.47 (t, 6H, meta, para), 5.63 (s, 2H, HN*H*), 4.21 [t, 4H, (C═O)-O-C*H*$_2$], 3.69−3.58 (m, CH_2 PEG), 3.42 [t, 4H, (C═O)-NH-C*H*$_2$ PEG], 3.13 [t, 4H, (C═O)-NH-C*H*$_2$ UAT], 1.7−1.3 [m, 16H, O═C═N−CH_2-(C*H*$_2$)$_4$-CH_2-NH]. Mass (MALDI-TOF MS): m/z = 1961.9 (M, PEG M_w = 1251.5 g/mol, UAT M_w = 355 g/mol (2×), PEG−(UAT)$_2$ M_w = 1961.5). FT-IR: 3500 ($\nu_{(OH)\ H\text{-bond}}$, w), 3400 ($\nu_{NH,1^o amine}$, w), 3300−3200 ($\nu_{NH,2^o amine}$, w), 2959−2882 ($\nu_{CH_2}$, w), 1739 ($\nu_{C=O\ ester}$, w), 1711 ($\nu_{C=O}$, w), 1630 ($\nu_{C=O\ amide}$, w), 1543 ($\nu_{NH,amide\ II}$, w), 1454−1466 ($\nu_{CH_2}$, m), 1280 ($\nu_{C-O/C-N}$, w), 1240 ($\nu_{C-O}$, w), 1239 ($\nu_{C-O-C}$, w), 1101 ($\nu_{C-O-C}$, s), 1060 ($\nu_{C-O-C}$, s), 952 ($\nu_{CH_2}$, m), 841 ($\nu_{C-O-C}$, ν_{CH_2}, m), and 528 cm^{-1} (ν_{CH_2}, w).

Sample Preparation. Gold substrates (200 nm gold on top of 3.5 nm Ti deposited onto glass substrates) were purchased from Ssens BV (Hengelo, The Netherlands). Prior to use, these substrates were cleaned in piranha solution [2:1 H_2SO_4 (Sigma−Aldrich)/H_2O_2 (30%, Fluka) by volume], then rinsed three times with Milli-Q water and ethanol, and subsequently rinsed with dichloromethane and chloroform, respectively. The samples were directly transferred to the monolayer solution, preventing any direct contact with air. ***Caution:*** *Piranha solution should be handled with extreme caution. It has been reported to detonate unexpectedly.* On gold substrates, self-assembled monolayers (SAMs)

dx.doi.org/10.1021/jp2089752 |*J. Phys. Chem. B* 2012, 116, 565–570

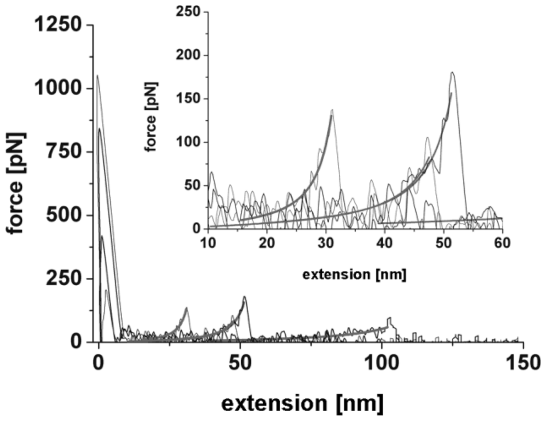

Figure 2. Force-extension curves acquired in the presence of bis(UAT) **3**. The curves were fitted to the wormlike chain (WLC) model, which provided the persistence length l_p = 3.63 ± 0.40 Å.

of **1** were prepared from 1 mM CH_2Cl_2 solution and reacted with 2.5 mmol of **2** in 10 mL of $CHCl_3$ solution for 24 h, with one drop of dibutyltin dilaurate as catalyst. After the SAM was rinsed with pure solvent and dried in an N_2 stream, measurements were performed with minimal delay. The same procedure was used for AFM tip functionalization.

General Characterization Methods. ^{1}H NMR spectra were recorded on a Varian Unity 300 spectrometer. Spectra (300 MHz) were recorded in $CDCl_3$ and therefore chemical shifts are given relative to the residual $CHCl_3$ peak (7.26 ppm). ^{1}H NMR on polymers was performed on a Bruker 600 MHz instrument. FT-IR bulk measurements were performed on a Bruker Alpha-P setup. The mass of the bifunctional PEG−$(UAT)_2$ linker was analyzed with matrix-assisted laser desorption ionization time-of-flight (MALDI-TOF) spectrometry on an Applied Biosystems Voyager DE-RP unit.

Atomic Force Microscopy. AFM-SMFS measurements were performed on a Veeco/Bruker Multimode (NanoScope V controller, Veeco/Bruker, Santa Barbara, CA) with a Picoforce vertical

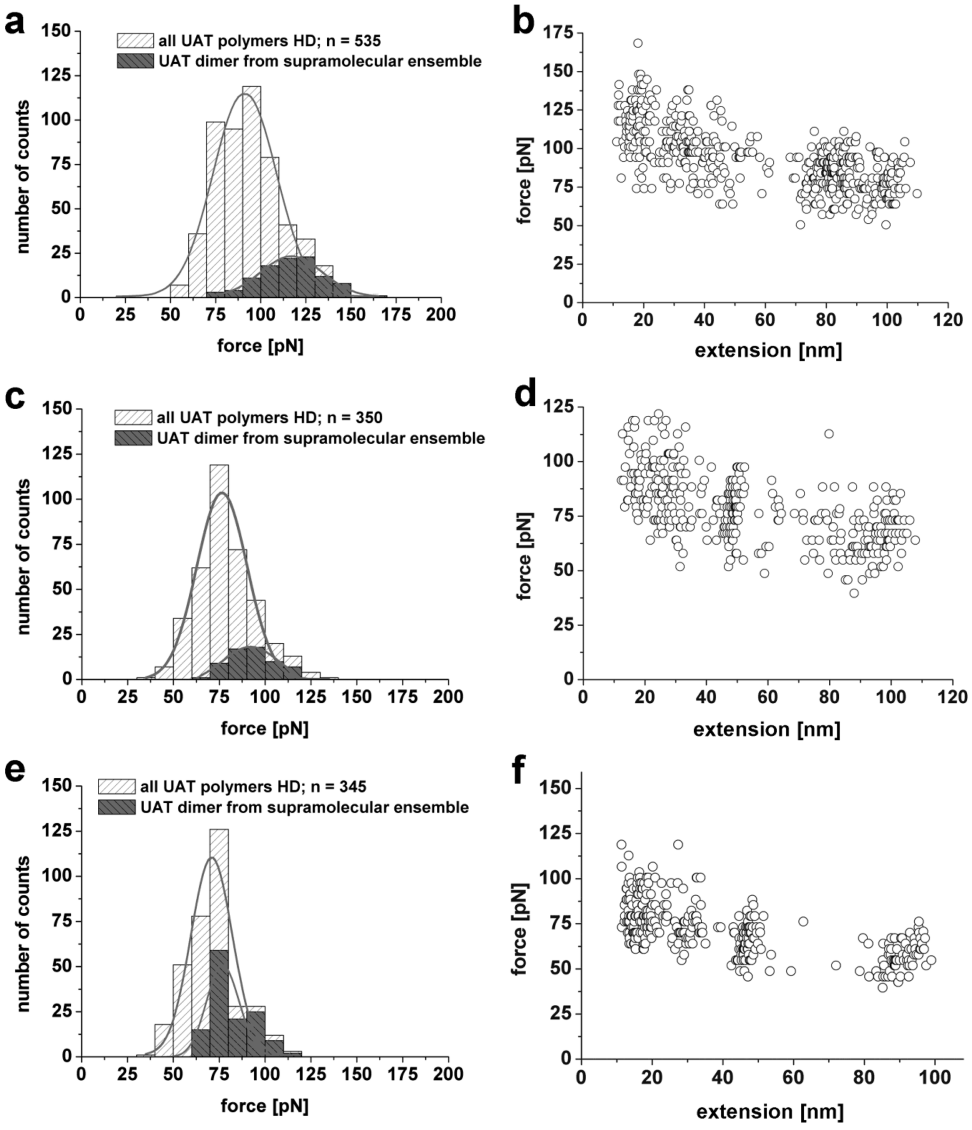

Figure 3. Histograms of rupture forces (left, a, c, e) and plots of rupture force vs length for unbinding in hexadecane (right, b, d, f) at the following loading rates: (a, b) r = (121 ± 28) nN/s; (c, d) r = (68 ± 21) n/s; (e, f) r = (32 ± 7) nN/s. Note that the dimer rupture events (assigned to unbinding events with stretch lengths between 11 and 22 nm, black) in all histograms display a substantially higher most probable unbinding force compared to the ensemble of all supramolecular polymer unbinding events (gray) for a specific loading rate.

dx.doi.org/10.1021/jp2089752 |J. Phys. Chem. B 2012, 116, 565–570

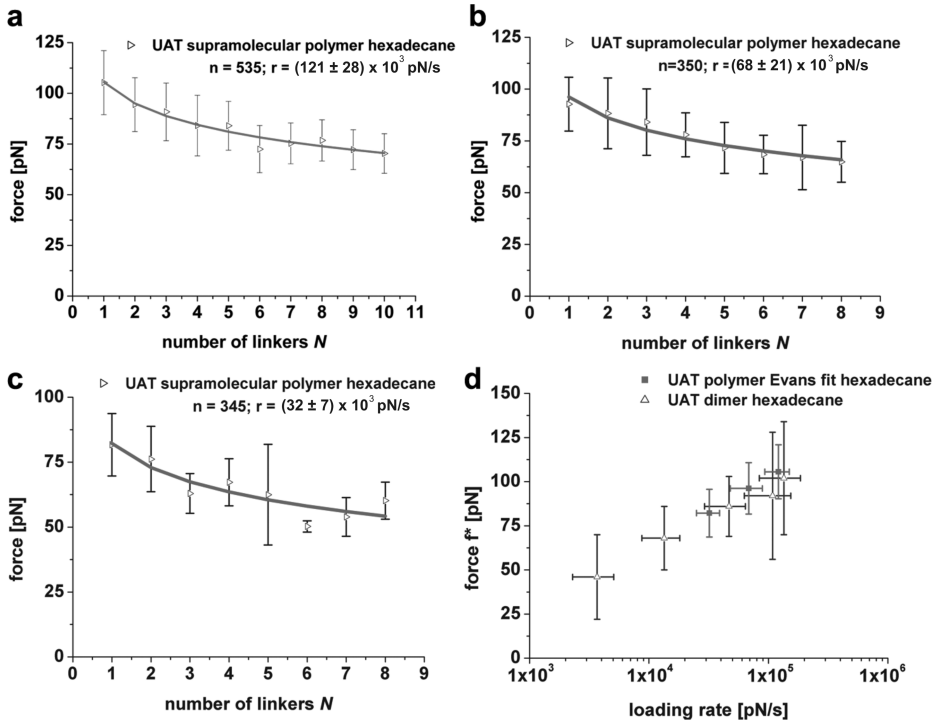

Figure 4. (a–c) Plots of most probable rupture forces vs N and fits to the model for uncooperative bond failure in series for supramolecular polymers in hexadecane at fixed loading rates: (a) $r = (121 \pm 28)$ nN/s, $f_\beta = 15.3 \pm 1.6$ pN, $f^*_{single} = 105.6 \pm 2.4$ pN; (b) $r = (68 \pm 21)$ nN/s, $f_\beta = 14.6 \pm 1.4$ pN, $f^*_{single} = 96.2 \pm 2.1$ pN; (c) $r = (32 \pm 7)$ nN/s, $f_\beta = 13.5 \pm 2.7$ pN, $f^*_{single} = 82.2 \pm 2.1$ pN; (d) comparison of data from the dimer rupture study[10] with fits obtained in this study of the most probable dimer rupture force f^*_{single}.

engage scanner and a liquid cell (Bruker/Veeco, Santa Barbara, CA). A double-side gold-coated MikroMasch rectangular beam cantilever (CSC38) was functionalized in two consecutive steps, as described above, with a self-assembled layer of **1** and subsequent reaction with **2**. The functionalized probe was taken directly from solution followed by rinsing with pure solvent. The cantilever spring constant ($k = 0.133 \pm 0.014$ N/m) was determined in liquid via the thermal tune method.[16] All experiments were performed in a saturated solution of **3** in anhydrous hexadecane at $T = 303 \pm 2$ K, concentration = 2.5×10^{-5} M.

RESULTS AND DISCUSSION

To determine the rupture forces of supramolecular UAT polymers in hexadecane, a PEG–UAT-functionalized gold surface and gold-coated AFM probe were used as described in ref 10. Additionally the bis(UAT)PEG linker **3** (Scheme 1) was added to the solution in a concentration of 2.5×10^{-5} M to result in the formation of supramolecular UAT polymers in situ (Figure 1). By use of AFM-SMFS, supramolecular polymer chains, which bridged between the sample and the AFM tip surfaces, were stretched and broken at three different but *fixed* loading rates. The loading rates used ensure far-from-equilibrium conditions:[10] $r = (32 \pm 7)$, (68 ± 21), and (121 ± 28) nN/s.

Since PEG linkers with a molar mass $M_w = 1250$ g/mol (bis-functionalized) and $M_w = 1500$ g/mol were used (monofunctionalized), the stretch length of the hydrogen-bonded moiety is known a priori (11 nm per linker unit[17]) and hence the number linkers N can be determined. As can be seen in Figure 2, the rupture lengths observed exceeded those expected (and observed)[10] for the dimers significantly. Since these rupture lengths were observed only in the presence of **3**, the formation of supramolecular polymer chains bridging between the substrate surface and the tip can be concluded. After the data were converted to force–extension curves (Figure 2), the rupture length and rupture force were determined.[18] The corresponding data are plotted in histograms for the three different but fixed loading rates used (Figure 3). Fitting the force–extension curves to the wormlike chain (WLC) model confirmed that indeed single-molecule supramolecular polymers were stretched. The wormlike chain fits provided a value for the persistence length of $l_p = 3.63 \pm 0.40$ Å, which is in good agreement with literature data.[19,20] On the basis of the length of the PEG linker and the attached UAT moieties of the bis(UAT) linker, the stretch length of each single supramolecular UAT polymer was converted to the number of linkers N: $N = (L/11\ \text{nm}) - 1$.

Hence the most probable force f^* was estimated and plotted as a function of N. As shown in Figure 4, the most probable rupture force f^* was found to decrease with the number of linkers N for all data sets.

Subsequently the data were fitted by use of a fast-converging Marquart-Levenberg algorithm to eq 3 for uncooperative bond rupture in series described by Evans and Williams. The fitted data for the three data sets (Figure 4) obtained at different but fixed loading rates, provided the most probable rupture force of the dimer f^*_{single} as well as the thermal scale force f_β. An overview of the obtained data is presented in Figure 4, where the error bars denote the standard deviation of the distribution. Subsequently the parameters for the potential energy landscape were determined. Analysis of three different data sets provided the data presented in Table 1. The parameters for the potential energy landscape of the $(UAT)_2$ bond were calculated as usual for a standard Evans approach, by use of eqs 1 and 2.

Table 1. Summary of Parameters Determined via AFM-SMFS of UAT Supramolecular Polymers in Hexadecane for Three Different but *Fixed* Loading Rates in Comparison with Loading Rate-Dependent Dimer Bond Rupture Studies

	polymer (32 ± 7) nN/s	polymer (68 ± 21) nN/s	polymer (121 ± 28) nN/s	dimer study[10]
f_β, pN	13.5 ± 2.7	14.6 ± 1.4	15.3 ± 1.6	14.5 ± 1.1
f^*_{single},[21] pN	82.2 ± 2.1	96.2 ± 2.1	105.6 ± 2.4	r_f-*dependent*
r^0_f, pN/s	(2.4 ± 1.9) × 10^2	(2.8 ± 1.4) × 10^2	(3.9 ± 2.1) × 10^2	(1.5 ± 0.9) × 10^2
$t_{off}(0)$ [ms]	130 ± 90	70 ± 30	50 ± 30	100 ± 80
x_β, nm	0.31 ± 0.08	0.29 ± 0.03	0.27 ± 0.04	0.29 ± 0.02

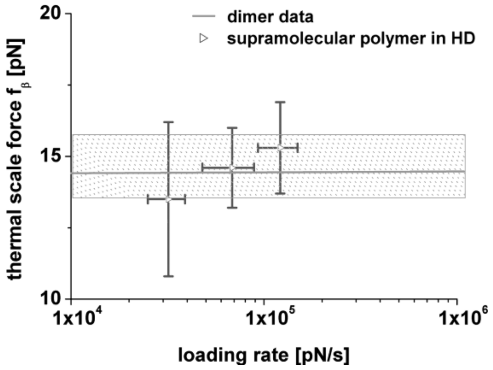

Figure 5. Plot of the thermal scale force f_β data obtained by unbinding studies of dimers (ref 10, shaded area) and supramolecular polymers (this study, data points) in hexadecane, including their error margins representing the standard deviation. Since a range of loading rates was used in ref 10 to determine the thermal scale force f_β, this is represented with a line and the corresponding error bar over the full range of loading rates.

Figure 4d provides a comparison of the fitted most probable rupture force of the dimers f^*_{single} (as part of the supramolecular ensemble, $N = 1$)[21] at the three different but fixed loading rates; the loading rate-dependent dimer studies in ref 10 are presented as well. As can be observed in Figure 4 (panel d) and Table 1, the fitted values obtained for the three different data sets - at a single fixed loading rate - and the corresponding parameters of the potential energy landscape, are in close agreement with each other. This result is even more evident if the two methods are compared with each other in the way that is presented in Figure 5.

On the basis of these results and considering the number of data points for each data set, an average kinetic off-time (or bond lifetime) t_{off} was calculated as 78 ± 64 ms. Furthermore, an average distance of the characteristic transition state along the unbinding trajectory x_β = 0.29 ± 0.05 was determined, which compares favorably to the hydrogen-bond distances (0.275−0.325 nm) reported by Beijer et al.[22] for these DADA dimers using crystallography.

If the available theoretical models[23] and solvent polarity trends for hydrogen-bond strength[24] are taken into account (which predict a dimer binding constant of $K_{dim} \approx 3 \times 10^4\ M^{-1}$) as well as a diffusion-limited association regime with $k_{on} = 10^8\ (M \cdot s)^{-1}$, a kinetic off-time $t_{off} \approx 0.3$ ms can be estimated (via $t_{off} = 1/k_{off}$). The mean value of t_{off} = 78 ± 64 ms, determined here by AFM-SMFS, is almost 3 orders of magnitude higher and can be attributed to an additional intramolecular stabilization, as was shown previously in the bulk on the basis of NMR experiments.[10] Furthermore, these results are close in line with bulk measurements obtained by Beijer et al.[22] for binding constants of various DADA hydrogen-bonded arrays in chloroform.

Finally, we emphasize the main advantage of our procedure: that is, the fact that only one single measured data set at one *fixed* loading rate is required to obtain all parameters of the potential energy landscape on a single-molecule level. Since the same procedure and equations are used to determine the parameters of the energy landscape of dimers, also similar errors are introduced. An additional error, which is only introduced by this approach, lies in the conversion of stretch length to number of linkers N. From eq 3 it can be concluded that the error in f_β depends linearly on the error in f^* for small N, and hence reasonable accuracy is obtained when large data sets with a substantial polymer length, such as those presented here, are used to determine f_β.

This central result fully validates our approach and shows that the choice of the loading rate possesses only negligible influence on the parameters estimated, as long as the unbinding events occur under far-from-equilibrium conditions.

CONCLUSIONS

The results presented here, combined with those presented in ref 12, show that the forced unbinding of single supramolecular polymers at one fixed piezo retraction rate in far-from-equilibrium conditions by AFM-SMFS provides all single-molecule rupture force parameters required to calculate kinetic off-rates and characteristic bond lengths. The measured rupture forces of novel UAT supramolecular polymers of different length and independent knowledge of the constituent segment length provided access to the dimer bond lifetime at zero force, $t_{off}(f = 0)$ = 78 ± 64 ms. For both types of supramolecular polymers investigated thus far (UPy and UAT), the results agree with previously obtained data for loading rate-dependent dimer interaction studies.[9,10] Furthermore, the results are well in line with actual measurements by Beijer et al.[22] of the dimer binding constant of the same or similar systems in chloroform and other organic solvents based on NMR binding studies (DADA) or fluorescence spectroscopy studies of pyrene-labeled UPy-moieties (DDAA).[24] Finally, these results demonstrate that the uncooperative bond failure model can be applied for strongly interacting systems for far-from-equilibrium conditions.

AUTHOR INFORMATION

Corresponding Author

*Fax (+49) 271 740 2805, e-mail schoenherr@chemie.uni-siegen.de (H.S.); fax (+31) 53 489 3823, e-mail g.j.vancso@utwente.nl (G.J.V.).

Present Addresses

[†]Department of Chemical Engineering, Section Nanostructured Materials, Delft University of Technology, Julianalaan 136, 2628 BL Delft, The Netherlands.

‡Department of Physical Chemistry I, University of Siegen, Adolf-Reichwein-Str. 2, 57076 Siegen, Germany.

■ ACKNOWLEDGMENT

This work has been financially supported by the Council for Chemical Sciences of The Netherlands Organization for Scientific Research (CW-NWO), ECHO Grant 754021, and NWO Middelgroot Grant 700.54.102. We thank Aleksandr Noy for stimulating and encouraging discussions.

■ REFERENCES

(1) (a) Brunsveld, L.; Folmer, B. J. B.; Meijer, E. W. *Chem. Rev.* **2001**, *101*, 4071–4097. (b) Bergman, S. D.; Wudl, F. *J. Mater. Chem.* **2008**, *18*, 41–62. (c) Montarnal, D.; Tournilhac, F.; Hidalgo, M.; Couturier, J.-L.; Leibler, L. *J. Am. Chem. Soc.* **2009**, *131*, 7966–7968.

(2) (a) Samori, P., Ed. *Scanning Probe Microscopies Beyond Imaging: Manipulation of Molecules and Nanostructures*; Wiley−VCH: Weinheim, Germany, 2006. (b) Schröder, T.; Geisler, T.; Walhorn, V.; Schnatwinkel, B.; Anselmetti, D.; Mattay, J. *Phys. Chem. Chem. Phys.* **2010**, *12*, 10981–10987. (c) Eckel, R.; Ros, R.; Decker, B.; Mattay, J.; Anselmetti, D. *Angew. Chem., Int. Ed.* **2005**, *44*, 484–488.

(3) (a) Gutiérrez-Medina, B.; Andreasson, J. O. L.; Greenleaf, W. J.; LaPorta, A.; Block, S. M. *Methods Enzymol.* **2010**, *475*, 377–404. (b) Kellerman, M. S. Z.; Smith, S. B.; Granzier, H. L.; Bustamante, C. *Science* **1997**, *276*, 1112–1116. (c) Ashkin, A.; Schutze, K.; Dziedzic, J. M.; Euteneuer, U.; Schliwa, M. *Nature* **1990**, *348*, 346–348.

(4) (a) Celedon, A.; Nodelman, I. M.; Wildt, B.; Dewan, R.; Searson, P.; Wirtz, D.; Bowman, G. D.; Sun, S. X. *Nat. Lett.* **2009**, *9*, 1720–1725. (b) Smith, S. B.; Finzi, L.; Bustamante, C. *Science* **1992**, *258*, 1122–1126.

(5) Evans, E.; Ritchie, K. In *Scanning Probe Microscopies and Molecular Materials*; Proceedings of the NATO Advanced Research Workshop, Tegernsee, Germany, May 29−June 3, 1994; Rabe, J., Gaub, H. E., Hansma, P. K., Eds.; Kluwer: Dordrecht, The Netherlands, 1994.

(6) Serpe, M. J.; Rivera, M.; Kersey, F. R.; Clark, R. L.; Craig, S. L. *Langmuir* **2008**, *24*, 4738–4742.

(7) (a) Puchner, E. M.; Gaub, H. E. *Angew. Chem., Int. Ed.* **2010**, *49*, 1147–1150. (b) Puchner, E. M.; Alexandrovich, A.; Kho, A. L.; Hensen, U.; Schäfer, L. V.; Brandmeier, B.; Gräter, F.; Grubmüller, H; Gaub, H. E.; Gautel, M. *Proc. Natl. Acad. Sci. U.S.A.* **2008**, *105*, 13385–13390.

(8) Aioanei, D.; Lv, S.; Tessari, I.; Rampioni, A.; Babacco, L.; Li, H.; Samori, B.; Brucale, M. *Angew. Chem., Int. Ed.* **2011**, *50*, 4394–4397.

(9) (a) Zou, S.; Schönherr, H.; Vancso, G. J. *J. Am. Chem. Soc.* **2005**, *127*, 11230–11231. (b) Zou, S.; Schönherr, H.; Vancso, G. J. *Angew. Chem., Int. Ed.* **2005**, *44*, 956–959.

(10) Embrechts, A.; Velders, A. H.; Schönherr, H.; Vancso, G. J. *Langmuir* **2011**, *27*, 14272–14278.

(11) (a) Bell, G. I. *Science* **1978**, *200*, 618–627. (b) Merkel, R.; Nassoy, P.; Leung, A.; Ritchie, K.; Evans, E. *Nature* **1999**, *397*, 50–53. (c) Evans, E. *Annu. Rev. Biophys. Biomol. Struct.* **2001**, *30*, 105–128.

(12) Embrechts, A.; Schönherr, H.; Vancso, G. J. *J. Phys. Chem B* **2008**, *112*, 7359–7362.

(13) Williams, P.; Evans, E. Dynamic Force Spectroscopy. In *Physics of Bio-Molecules and Cells*; Ecoles des Houches d'Eté LXXV; Julicher, F., Ormos, P., David, F., Flyvbjerg, H., Eds.; EDP Sciences/Springer Verlag: Berlin, 2002; pp 147-203.

(14) (a) Fugman, S.; Sokolov, I. M. *Phys. Rev. E* **2009**, *79*, No. 021803. (b) Fugman, S.; Sokolov, I. M. *EPL* **2009**, *86*, 28001.

(15) (a) Neises, B.; Steglich, W. *Org. Synth.* **1990**, *7*, 93–94. (b) Folmer, B. J. B.; Sijbesma, R. P.; Versteegen, R. M.; van der Rijt, J. A. J.; Meijer, E. W. *Adv. Mater.* **2000**, *12*, 874–878.

(16) Hutter, J. L.; Bechhöfer, J. *Rev. Sci. Instrum.* **1993**, *64*, 1868–1873.

(17) A monodisperse PEG-linker was used with n = 28. The monodispersity of the final bifunctional linker was confirmed by MALDI-TOF (see Materials and Methods). On the basis of the bond length between atoms of the complete structure and the number of PEG units, the total length of the bifunctional UAT linker can be determined as 11 nm. The error in the stretch length is very small in this case due to the low polydispersity (±0.3 nm for a difference in the PEG linker of one PEG unit).

(18) The conversion from deflection versus piezo position to force−distance curves was carried out by use of Veeco offline analysis software v730r1sr2 and v810r1sr1. Baseline correction and WLC fitting was subsequently achieved by use of Origin version 6.1. Stretch lengths and unbinding forces were determined by use of PUNIAS 3D. Loading rates were determined as the slope of the force versus time trace of the force−extension curves (∼20 data points) close to the rupture event (Origin 6.1).

(19) (a) Oesterhelt, F.; Rief, M.; Gaub, H. E. *New J. Phys.* **1999**, *1*, 6.1–6.11. (b) Kienberger, F.; Pastushenko, V. P.; Kada, G.; Gruber, H. J.; Riener, C.; Schindler, H.; Hinterdorfer, P. *Single Mol.* **2000**, *1*, 123–128.

(20) According to literature, the helical-state monomer length of PEG is 2.78 Å, and persistence length l_p = 3.81 ± 0.02 Å (WLC) and Kuhn length l_K = 7 Å [from a fit to the freely joined chain (FJC) model] were previously reported.[19] So the fitted persistence length agrees very well with literature, which confirms that *single supramolecular polymers* were probed. In our measurements, the difference between the elasticity parameters obtained from fits to the WLC and FJC models is negligible since small extensions at low rupture forces were studied. In that case the following expression for the relation of the persistence length and Kuhn length applies: $l_p = 1/2l_K$. Hence the average persistence length of l_p = 3.63 ± 0.40 Å is well in line with previously reported data and confirms that single chains were stretched and hence single-molecule rupture events were probed.

(21) The errors represented in Table 1 are the errors provided by the fit of the data to the uncooperative bond failure model; however, as a more physically relevant value for the standard deviation of the most probable rupture force, $\Delta f^* = f_\beta$ was used, based on the standard deviation for thermally activated unbinding events.[13]

(22) Beijer, F. H.; Kooijman, H.; Spek, A. L.; Sijbesma, R. P.; Meijer, E. W. *Angew. Chem., Int. Ed.* **1998**, *37*, 75–78.

(23) Sartorius, J.; Schneider, H.-J. *Chem.—Eur. J.* **1996**, *2*, 1446–1452.

(24) Söntjens, S. H. M.; Sijbesma, R. P.; Van Genderen, M. H. P.; Meijer, E. W. *J. Am. Chem. Soc.* **2000**, *122*, 7487–7493.